© 2015. Published by The Company of Biologists Ltd | Development (2015) 142, 2574-2585 doi:10.1242/dev.122630

RESEARCH ARTICLE

STEM CELLS AND REGENERATION

Fat4/Dchs1 signaling between stromal and cap mesenchyme cells influences nephrogenesis and ureteric bud branching

Yaopan Mao[1], Philippa Francis-West[2] and Kenneth D. Irvine[1,*]

ABSTRACT

Formation of the kidney requires reciprocal signaling among the ureteric tubules, cap mesenchyme and surrounding stromal mesenchyme to orchestrate complex morphogenetic events. The protocadherin Fat4 influences signaling from stromal to cap mesenchyme cells to regulate their differentiation into nephrons. Here, we characterize the role of a putative binding partner of Fat4, the protocadherin Dchs1. Mutation of *Dchs1* in mice leads to increased numbers of cap mesenchyme cells, which are abnormally arranged around the ureteric bud tips, and impairment of nephron morphogenesis. Mutation of *Dchs1* also reduces branching of the ureteric bud and impairs differentiation of ureteric bud tip cells into trunk cells. Genetically, *Dchs1* is required specifically within cap mesenchyme cells. The similarity of *Dchs1* phenotypes to stromal-less kidneys and to those of *Fat4* mutants implicates Dchs1 in Fat4-dependent stroma-to-cap mesenchyme signaling. Antibody staining of genetic mosaics reveals that Dchs1 protein localization is polarized within cap mesenchyme cells, where it accumulates at the interface with stromal cells, implying that it interacts directly with a stromal protein. Our observations identify a role for Fat4 and Dchs1 in signaling between cell layers, implicate Dchs1 as a Fat4 receptor for stromal signaling that is essential for kidney development, and establish that vertebrate Dchs1 can be molecularly polarized *in vivo*.

KEY WORDS: Dachsous, Fat, Kidney, Nephron

INTRODUCTION

Metanephric kidney development requires interactions between three adjacent cell layers: the epithelial ureteric bud (UB), the cap mesenchyme (CM) and the stromal mesenchyme (stroma) (Fig. 1A) (Costantini and Kopan, 2010; Kopan et al., 2014). The UB forms a tubule that undergoes elongation and reiterative branching to form the collecting ducts. Growth and branching of the UB depends upon reciprocal cell signaling interactions with the neighboring CM, which coalesces around the tips of the branching epithelium. CM cells are also the progenitor cells for nephrons, which are created through a mesenchymal-to-epithelial transition to form a renal vesicle, which then undergoes further growth and morphogenesis (Costantini and Kopan, 2010; Kopan et al., 2014). The CM is surrounded by stroma. Genetic ablation of stromal cells or mutation of stromal-expressed genes, including *Ecm1*, *Foxd1* and *Fat4*, has revealed that stroma influences the development of the CM and UB (Das et al., 2013; Hatini et al., 1996; Hum et al., 2014; Levinson et al., 2005; Paroly et al., 2013). Nonetheless, there remain substantial gaps in our understanding of the cellular and molecular mechanisms that orchestrate the communication between stromal cells and other cell layers required for kidney morphogenesis. Here, we examine the role of Dchs1/Fat4 signaling in this process.

Much of our understanding of Dchs1 and Fat4 comes from studies of their *Drosophila* homologs, Dachsous (Ds) and Fat. Ds and Fat are large cadherin family transmembrane proteins that bind to each other to regulate both Hippo signaling and planar cell polarity (PCP) (Matis and Axelrod, 2013; Reddy and Irvine, 2008; Staley and Irvine, 2012; Thomas and Strutt, 2012). Hippo signaling is a conserved signal transduction pathway best known for its influence on organ growth, which it controls by regulating a transcriptional co-activator protein called Yorkie (Yki), or in vertebrates the Yki homologs Yap and Taz (Pan, 2010; Staley and Irvine, 2012). PCP is the polarization of cell morphology and cell behavior within the plane of a tissue (Goodrich and Strutt, 2011; Wansleeben and Meijlink, 2011). PCP signaling is intrinsically bidirectional, as it polarizes each pair of juxtaposed cells. Conversely in Fat/Hippo signaling, Ds acts as a ligand that activates Fat, which functions as a receptor for Hippo signaling (Reddy and Irvine, 2008; Staley and Irvine, 2012), but there is also some evidence for a reciprocal Fat-to-Ds signal (Degoutin et al., 2013).

Analysis of *Fat4* and *Dchs1* mutant mice has revealed that Dchs1/Fat4 signaling is essential for the morphogenesis of multiple mammalian organs, including the kidney (Mao et al., 2011; Saburi et al., 2008, 2012; Zakaria et al., 2014). Requirements for *DCHS1* and *FAT4* in humans have been revealed by the linkage of mutations in these genes to Van Maldergem syndrome (Cappello et al., 2013). Mice mutant for *Dchs1* or *Fat4* have smaller kidneys, with fewer ureteric branches and a modest accumulation of small cysts (Mao et al., 2011; Saburi et al., 2008); hypoplastic kidneys have also been reported in Van Maldergem patients (Mansour et al., 2012). Differences between murine wild-type and *Dchs1* or *Fat4* mutant kidneys appear as early as embryonic day (E) 11.5, when the growth and branching of the UB in mutants lags behind that in wild-type embryos (Mao et al., 2011).

Differentiation of nephron progenitor cells (CM) into nephrons was reported to be defective in *Fat4* mutants (Das et al., 2013), reminiscent of the effect of stromal cell ablation on CM differentiation (Das et al., 2013; Hum et al., 2014), and it was suggested that Fat4 participates in stromal-to-CM signaling. The inhibition of nephron progenitor cell differentiation in *Fat4* mutants was attributed to increased Yap activity (Das et al., 2013), although how this might be achieved is unclear, as the molecular pathway linking Fat to Yap identified in *Drosophila* does not appear to be conserved in mammals (Bossuyt et al., 2014; Pan et al., 2013). Conversely, there is growing evidence that Ds/Fat PCP signaling mechanisms are conserved between insects and vertebrates,

[1]Howard Hughes Medical Institute, Waksman Institute and Department of Molecular Biology and Biochemistry, Rutgers University, Piscataway, NJ 08854, USA. [2]Department of Craniofacial Development and Stem Cell Biology, King's College London, Floor 27, Guy's Tower, London SE1 9RT, UK.

*Author for correspondence (irvine@waksman.rutgers.edu)

Received 28 January 2015; Accepted 18 June 2015

Development (2015) 142, 2574-2585 doi:10.1242/dev.122630

including the ability of human FAT4 to rescue PCP phenotypes in flies (Pan et al., 2013) and observations of abnormal cellular polarization in *Dchs1* or *Fat4* mutant mice (Mao et al., 2011; Saburi et al., 2008; Zakaria et al., 2014).

Here, we focus on the role of *Dchs1* in mouse kidney development. We report that *Dchs1* mutants share the expansion of CM identified in *Fat4* mutants, consistent with the hypothesis that they act as a signaling pair. We also further characterize *Dchs1* phenotypes in other cell types within the kidney, and show through conditional deletion that *Dchs1* is specifically required within CM for the normal development of CM, UB and stroma. Analysis of genetic mosaics establishes that the subcellular localization of Dchs1 is polarized within CM cells, where it accumulates on surfaces contacting stromal cells. Our observations suggest that Dchs1 functions as a receptor for a Fat4 signal from stromal cells that influences the behavior of CM and, indirectly, that of the UB.

RESULTS

Dchs1 functions in CM to influence kidney size and shape

Immunolocalization and RNA *in situ* studies of E12.5 kidneys revealed that Fat4 and Dchs1 are expressed predominantly within the CM and stroma, rather than in the UB (Mao et al., 2011). Similarly, Fat4 and Dchs1 protein expression could be readily detected within the CM and stroma of E14.5 kidneys (Fig. 1B,D), whereas the UB appears to have levels of staining close to background (i.e. similar levels to those as observed in mutant kidneys, Fig. 1C,E). These observations raise the question of how Fat4 and Dchs1 influence UB branching and growth. To determine where *Dchs1* is genetically required for kidney development, we selectively removed *Dchs1* from each of the three main cell types within the developing kidney by using a *Dchs1* conditional allele (*Dchs1*^{f}) combined with either *Hoxb7-Cre* (expressed in UB) (Yu et al., 2002), *Foxd1-Cre* (expressed in stroma) (Humphreys et al., 2010) or *Six2-Cre* (expressed in CM and immediate derivatives) (Kobayashi et al., 2008). The efficacy and specificity of these Cre lines was confirmed using a conditional *Rosa-26 lacZ* reporter (Soriano, 1999) (supplementary material Fig. S1) and by Dchs1 antibody staining (see below).

When kidneys from postnatal day (P) 0 mice with conditional deletion of *Dchs1* in stromal cells or in the UB were examined, they appeared morphologically normal in terms of overall kidney size and shape (Fig. 1F-I,L,M,O,P). Conversely, conditional deletion of *Dchs1* from CM resulted in smaller, rounder kidneys, reminiscent of those observed in *Dchs1* mutant mice (Fig. 1J,K,N,Q) (Mao et al., 2011). Thus, *Dchs1* is required in CM or its derivatives for overall kidney growth, but not in UB or stroma.

Influence of *Dchs1* on CM

In developing wild-type kidneys, mesenchymal cells condense to form a two- to three-cell-wide cap around the UB tips; this cap is marked by strong expression of Six2 (Fig. 2A,C,E,G) (Kobayashi et al., 2008). Mutation of *Fat4* results in increased numbers of CM cells around each ureteric bud tip (Fig. 2B,F) (Das et al., 2013). *Dchs1* mutants exhibit a similar expansion of CM (Fig. 2D,H), consistent with inferences that Dchs1 and Fat4 function as signaling partners (Mao et al., 2011; Zakaria et al., 2014). In addition to the increase in thickness of the CM, the CM also appears disorganized in both *Dchs1* and *Fat4*, i.e. the width and shape of the cap appears more irregular than in wild type (Fig. 2A-H). Moreover, some CM cells appear to be mislocalized. In wild type they are restricted to the distal side of the ureteric tips, near the surface of the kidney, but in mutants they can accumulate proximal to the ureteric tips (Fig. 2A-D). Increased thickness and disorganization of CM has also been noted in kidneys with stromal deletion, or mutation of *Ecm1*, *Foxd1* or *Fat4* (Das et al., 2013; Hatini et al., 1996; Hum et al., 2014; Levinson et al., 2005; Paroly et al., 2013).

To investigate the origin of these defects in CM thickness and organization, we examined CM cells in *Fat4* mutants throughout kidney development, beginning at E10.5 when the ureteric epithelium first invades the metanephric mesenchyme. At E11.5, the thickness of cap mesenchyme cells appears similar between wild-type and mutant kidneys (Fig. 2I,J), whereas by E12.5 the CM of *Fat4* mutants is clearly abnormal (Fig. 2K,L). Abnormalities in kidney morphogenesis nonetheless appear by E11.5 (Mao et al., 2011), and one intriguing difference revealed by Six2 staining is that in *Fat4* mutants the end of the UB remains completely surrounded by CM, whereas in wild type, as the UB elongates, regions of the UB not at the tip (the UB stalk) are no longer directly in contact with Six2-expressing CM (Fig. 2I,J).

To quantify the local increase in CM, we compared the volume of Cited1-expressing cells per UB tip in *Fat4* mutant and wild-type kidneys at E14.5; a threefold increase was observed in the mutants (Fig. 2Q). This was not associated with a detectable increase in CM cell proliferation (Fig. 2R-T). We also note that the local increase in CM around each UB tip does not correspond to an increase in total CM within the kidney, because there are fewer, more widely spaced, UB tips. This is illustrated by the observation that total Six2 expression, as measured by quantitative reverse-transcription PCR (Q-PCR), normalized to kidney size (using a ubiquitously expressed gene, GAPDH, as a Q-PCR standard) was similar in wild-type and *Fat4* mutant kidneys (110% of wild type; Fig. 3A). The observation that the total amount of CM is similar in wild-type and mutant kidneys (when normalized for kidney size) raises the question of whether Dchs1/Fat4 signaling has a specific effect on CM, or if the increased CM at UB tips might simply reflect a similar amount of CM distributed amongst fewer tips. We do not favor this latter possibility, because the CM and UB tips normally engage in reciprocal signaling to maintain their fates (Kopan et al., 2014). Additionally, we note that *Vangl2*^{Lp} mutants also have smaller kidneys with reduced branching (Yates et al., 2010), but they do not exhibit the expansion of CM observed in *Dchs1* or *Fat4* mutants (supplementary material Fig. S2E,F).

To determine where *Dchs1* functions to influence CM cells, we examined kidneys with conditional deletion of *Dchs1* in each of the three main cell types present within the early kidney. The expansion and irregular shape of CM was visible in kidneys with conditional deletion of *Dchs1* in CM (*Six2-Cre Dchs1*$^{f/-}$; Fig. 2M-P). The phenotype appears to be less severe than in *Dchs1* null mutants, but this probably reflects perdurance of Dchs1 mRNA and protein after conditional deletion of the gene, as Six2 expression in the kidney only begins at ∼E10.5 (Oliver et al., 1995). No effect on CM thickness or organization could be detected in kidneys with conditional deletion of *Dchs1* in stroma or UB (supplementary material Fig. S2A-D). Thus, *Dchs1* is required within the CM to influence CM thickness and organization.

Influence of Dchs1/Fat4 signaling on UB development

The smaller size of *Dchs1* and *Fat4* mutant kidneys correlates with reduced branching of the UB (Mao et al., 2011). Based on the density of UB tips in E14-E15 kidneys, branching is reduced by deletion of *Dchs1* in CM, but not UB or stroma (Fig. 2P; supplementary material Fig. S2A-D). Reduced branching was confirmed by counting all tips in E12.5 kidneys from mice with

Development (2015) 142, 2574-2585 doi:10.1242/dev.122630

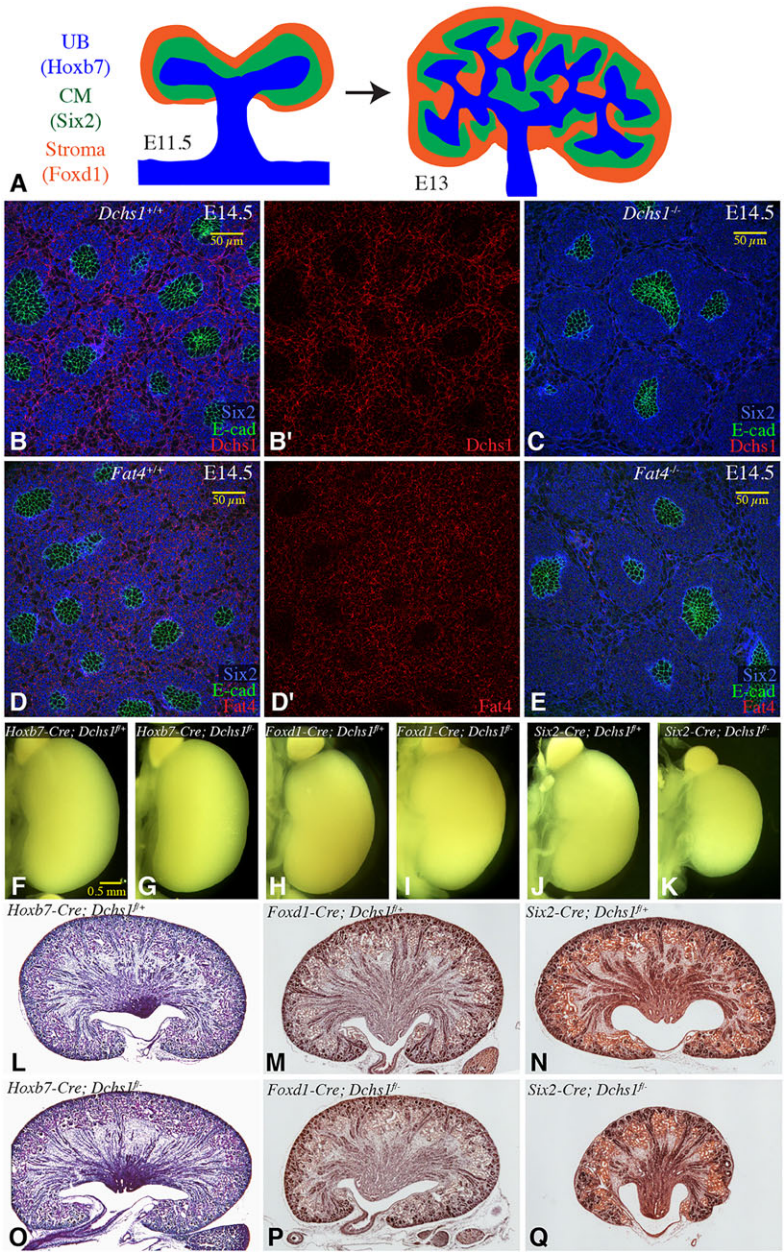

Fig. 1. Dchs1 functions in cap mesenchyme. (A) Schematic view of relative localization of stroma (orange), UB (blue) and CM (green) in embryonic kidneys at E11.5 (left) and E13 (right). Foxd1, Hoxb7 and Six2 are specifically expressed in these populations, as indicated. (B-E) Confocal images of E14.5 kidney surfaces showing Dchs1 (red, B,B′) and Fat4 (red, D,D′) protein expression, with CM and UB stained by Six2 (blue) and E-cad (green) antisera, respectively. Staining of *Dchs1* (C) or *Fat4* (E) mutant kidneys is shown to confirm antisera specificity. (F-Q) Representative examples (from at least three mice per genotype) of whole P0 kidneys (F-K) or Hematoxylin & Eosin-stained sections (L-Q) with conditional deletion (floxed allele over null allele) of *Dchs1* in stroma (Foxd1-Cre; I,P), UB (Hoxb7-Cre; G,O) or CM (Six2-Cre; K,Q), compared with sibling controls (floxed allele over wild type, F,H,J,L-N).

conditional deletion of *Dchs1* in *Six2*-expressing cells (*Six2-Cre Dchs1*$^{f/-}$), compared with heterozygous controls (*Six2-Cre Dchs1*$^{f/+}$) (Fig. 3B,D,E). This reduction is less than that observed when comparing null animals with wild-type siblings (Mao et al., 2011), but this could stem from a lag in loss of *Dchs1* after conditional deletion, and as deletion of *Dchs1* within UB or stroma had no detectable effect on kidney development, we conclude that *Dchs1* function within CM influences the growth and branching of the neighboring UB.

The observations that Dchs1 and Fat4 are predominantly expressed in CM and stroma, and that *Dchs1* is genetically required in CM, raises the question of how they influence branching of the UB. The UB can be subdivided into distinct cell types based on cell behavior and molecular markers. One fundamental subdivision is between tip cells and non-tip (trunk) cells. Tip cells engage in reciprocal signaling with cap mesenchyme cells to maintain their respective fates (Costantini and Kopan, 2010; Dressler, 2009; Kopan et al., 2014). For example, tip cells express Wnt ligands, including Wnt9b and Wnt11, that signal to CM, whereas CM cells express regulators of Ret and FGF signaling, including GDNF and FGFs, that signal to tip cells. Dchs1/Fat4 signaling is not required for this feedback loop per se, because Gdnf, Ret and Wnt 11 expression levels are all similar between wild-type and mutant kidneys (Fig. 3A) (Mao et al., 2011). However, the local expansion of CM in *Dchs1* and *Fat4* mutants could potentially increase the number of UB cells exposed to signals from CM, thereby increasing the population of ureteric cells specified as tip rather than trunk. To evaluate this hypothesis, we examined a tip cell marker, Sox9, in *Fat4* mutant kidneys versus wild-type kidneys. Indeed, an increase in Sox9-expressing cells could be observed at ureteric bud tips (Fig. 3C,F-I). This expansion in Sox9-expressing cells correlates with loss of staining of a trunk cell marker, the lectin *Dolichos biflorus* agglutinin (DBA) (Fig. 3J,K). We also quantified the expression levels of genes expressed in tip and trunk cells by Q-PCR (Fig. 3A). Two tip genes, Six2 and Ret, were expressed at similar levels between wild-type and mutant kidneys (Fig. 3A)

Development (2015) 142, 2574-2585 doi:10.1242/dev.122630

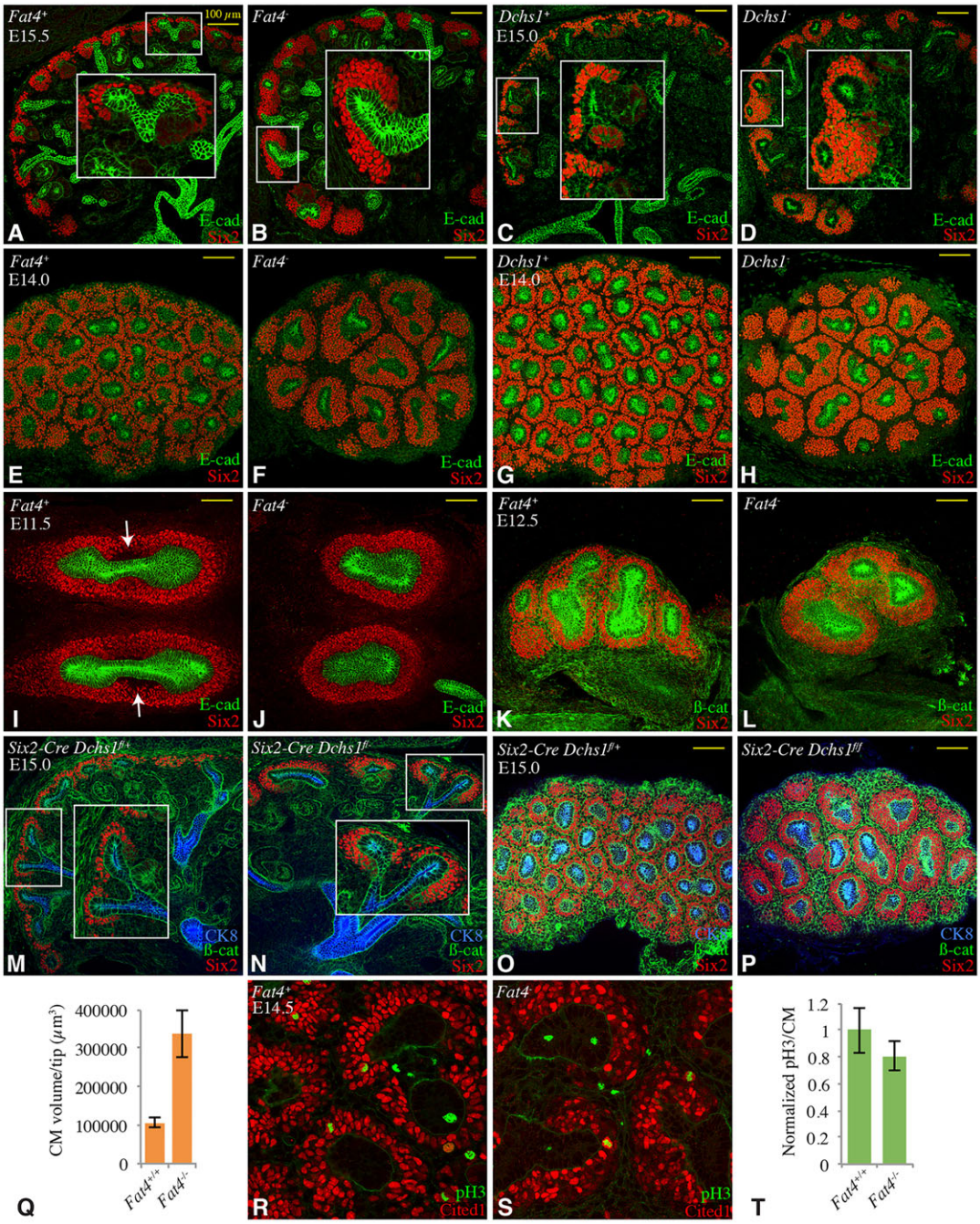

Fig. 2. Influence of *Dchs1* or *Fat4* mutation on cap mesenchyme. (A-P) Mutant and sibling control embryonic kidneys stained for Six2 (red, to reveal CM), together with E-cad (green, expressed in UB), β-cat (green, expressed in all cells), and/or CK8 (blue, expressed in UB). Scale bars: 100 µm. (A-D) Sagittal sections of E15.5 (A,B) or E15 (C,D) wild-type (A), *Fat4*$^{-/-}$ (B), wild-type (C) and *Dchs1*$^{-/-}$ (D) kidneys. Large boxed insets show higher magnification of the smaller boxed regions. (E-H) Surface sections of E14 wild-type (E), *Fat4*$^{-/-}$(F), wild-type (G) and *Dchs1*$^{-/-}$ (H) kidneys. (I,J) Confocal sections of E11.5 wild-type (I) and *Fat4*$^{-/-}$ (J) kidneys. Arrows point to trunk regions of the UB not contacted by CM. (K,L) Confocal sections of E12.5 wild-type (K) and *Fat4*$^{-/-}$(L) kidneys. (M-P) Sagittal (M,N) or surface (O,P) sections of E15 kidneys with conditional deletion of *Dchs1* in CM (*Six2-Cre Dchs1*$^{fl/d}$ or *Dchs1*$^{fl/f}$), or sibling controls (*Six2-Cre Dchs1*$^{fl/+}$). Larger insets show higher magnification of the smaller boxed regions. (Q) Quantification of mean CM volume per UB tip in *Fat4* mutant kidneys and wild-type siblings at E14.5, based on analysis of a Cited1-tagRFP reporter in six kidneys per genotype. (R,S) Examples of pH3 staining (green) for quantification of proliferation in CM (Cited1, red) in *Fat4* mutant (S) and wild-type siblings (R) at E14.5. (T) Quantification of proliferation in *Fat4* mutant CM (Cited1-expressing) and wild-type siblings at E14.5, based on counting pH3-positive cells per unit volume in nine kidneys per genotype, normalized to the proliferation index in wild-type CM. Error bars show 95% confidence intervals.

(Mao et al., 2011). However, E-cad (Cdh1 – Mouse Genome Informatics) levels were reduced (to 70% of wild type) in *Fat4* mutant kidneys (Fig. 3A). We interpret this as stemming from the reduction in the fraction of the kidney that comprises the UB (E-cad-expressing cells), consistent with the reduced branching and more widely spaced UB tips observed by confocal microscopy. Taken together, this Q-PCR analysis implies that the fraction of the UB system comprising tip cells (i.e. Sox9- and Ret-expressing cells) is increased in mutants. Direct examination of a trunk marker (Wnt7b) revealed a modest reduction in RNA levels (to 88% of wild

Development (2015) 142, 2574-2585 doi:10.1242/dev.122630

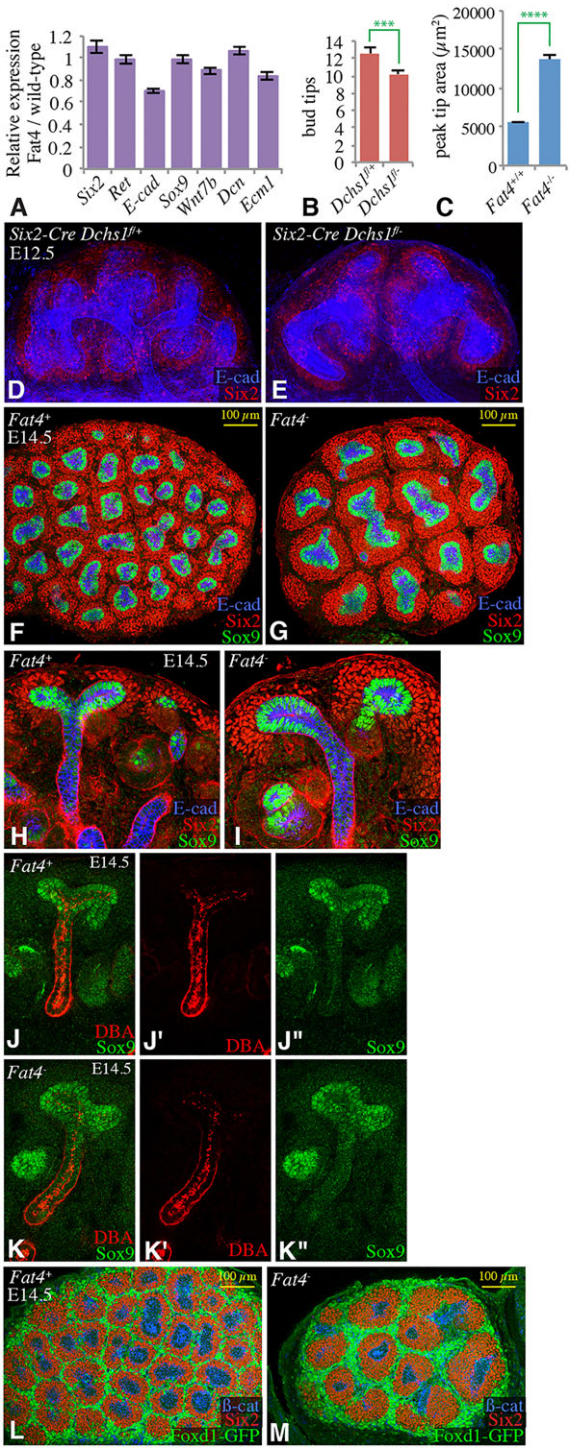

Fig. 3. Influence of *Dchs1* or *Fat4* mutation on UB and stroma. (A) Relative expression, by Q-PCR, of the indicated genes in E14.5 *Fat4* mutant versus wild-type kidneys, using *Gapdh* as a standard; three replicates were performed. Error bars indicate s.d. (B) Histogram showing average number of bud tips in E12.5 kidneys with conditional deletion of *Dchs1* in CM, or sibling controls (n=12 kidneys for each genotype). (C) Mean tip area (defined by Sox9 staining) in surface sections of E14.5 *Fat4* mutant or sibling control kidneys at maximum tip width (n=7 for control, 6 for mutant). Error bars for B and C indicate s.e.m., and significance was determined by t-test; ***$P\leq0.001$, ****$P\leq0.0001$. (D,E) Examples of confocal projections through whole E12.5 control (D; *Six2-Cre Dchs1*$^{fl/+}$) or conditional deletion (E; *Six2-Cre Dchs1*$^{fl/-}$) kidneys, stained for E-cad (blue) and Six2 (red). (F,G) Surface section through sibling control (F) and *Fat4*$^{-/-}$ (G) E14.5 kidneys stained for E-cad (blue), Six2 (red) and Sox9 (green). (H,I) Section through sibling control (H) and *Fat4*$^{-/-}$ (I) E14.5 UB tip and trunk stained for E-cad, Six2 and Sox9. (J-K″) Section through sibling control (J) and *Fat4*$^{-/-}$ (K) E14.5 UB tip and trunk stained for DBA (red) and Sox9 (green). Panels marked by prime symbols show individual stains. (L,M) Surface section through sibling control (L) and *Fat4*$^{-/-}$ (M) E14.5 kidneys imaged for β-cat (blue), Six2 (red) and Foxd1-GFP (green).

type; Fig. 3A). Altogether, these observations are consistent with the hypothesis that the branching defects in *Dchs1* and *Fat4* could arise as a secondary consequence of the expansion of CM and a promotion of tip cell fate in neighboring UB cells, which could then delay the formation of new branches.

Influence of *Dchs1* and *Fat4* on stromal cells

Despite the increased thickness of the CM, the space between clusters of CM is increased in *Dchs1* and *Fat4* mutants (Fig. 2E-H), concomitant with the decreased branching of the UB. The space between CM is normally occupied by Foxd1-expressing stromal cells. To assess the identity of intervening cells in *Dchs1* and *Fat4* mutant embryos, a transgene expressing GFP under Foxd1 control was examined in E14.5 *Dchs1* or *Fat4* mutant kidneys. This revealed that the intervening space between CM is filled with Foxd1-expressing stromal cells in both wild type and mutants (Fig. 3L,M; supplementary material Fig. S2G,H). As the space between clusters of CM remains as narrow as in wild type after conditional deletion of *Dchs1* in the UB or stroma (supplementary material Fig. S2A-D), but not after deletion of *Dchs1* in CM (Fig. 2P), we infer that this stromal cell phenotype also stems from the requirement for *Dchs1* in CM. This local expansion in stroma might simply reflect a similar number of Foxd1-expressing cells filling an expanded space between CM within a smaller mutant kidney.

Alternatively, it could be that Dchs1-Fat4-dependent signals specifically influence stromal cells. The continued expression of Foxd1 implies that normal stromal cell fate does not require Dchs1/Fat4 signaling. We also examined the expression of two genes that act in stromal cells to influence kidney development. Extracellular matrix 1 (*Ecm1*) is expressed by stromal cells in response to retinoic acid signaling, and influences UB branching at least in part by restricting Ret expression to UB tips (Paroly et al., 2013). Decorin (Dcn) expression is normally repressed by Foxd1 in stromal cells, and misexpression of Dcn contributes to the *Foxd1* mutant kidney phenotype (Fetting et al., 2014). However, Q-PCR analysis revealed that both of these genes are expressed at similar levels in wild-type and mutant kidneys (Ecm1 at 84% of wild type, Dcn at 107% of wild type; Fig. 3A).

Abnormal nephrogenesis in *Dchs1* and *Fat4* mutants

During early stages of nephrogenesis, CM cells condense to form a pre-cellular aggregate (PA), undergo a mesenchymal-to-epithelial transition to form a renal vesicle (RV), which as it begins to elongate into the nephron tubules transitions through distinctive comma-shaped body (CB) and S-shaped body (SB) stages (supplementary material Fig. S3A). Further elongation and morphogenesis establishes the nephron tubules and glomeruli. Das et al. (2013) reported that nephron differentiation was severely impaired in stroma-less kidneys or *Fat4* mutants. By contrast, Hum et al. (2014) reported that stroma-less kidneys had a similar extent of nephron differentiation as did controls, but that differentiated nephron structures were mispositioned. Using Wt1 as a marker, which stains CM, distal regions of the RV, CB and SB, and podocytes, we observed that nephron differentiation still occurs in *Fat4* mutants, as visualized by the appearance of Wt1-expressing podocytes (Fig. 4A,B). However, there are abnormalities in early nephron morphogenesis. The shape of

Development (2015) 142, 2574-2585 doi:10.1242/dev.122630

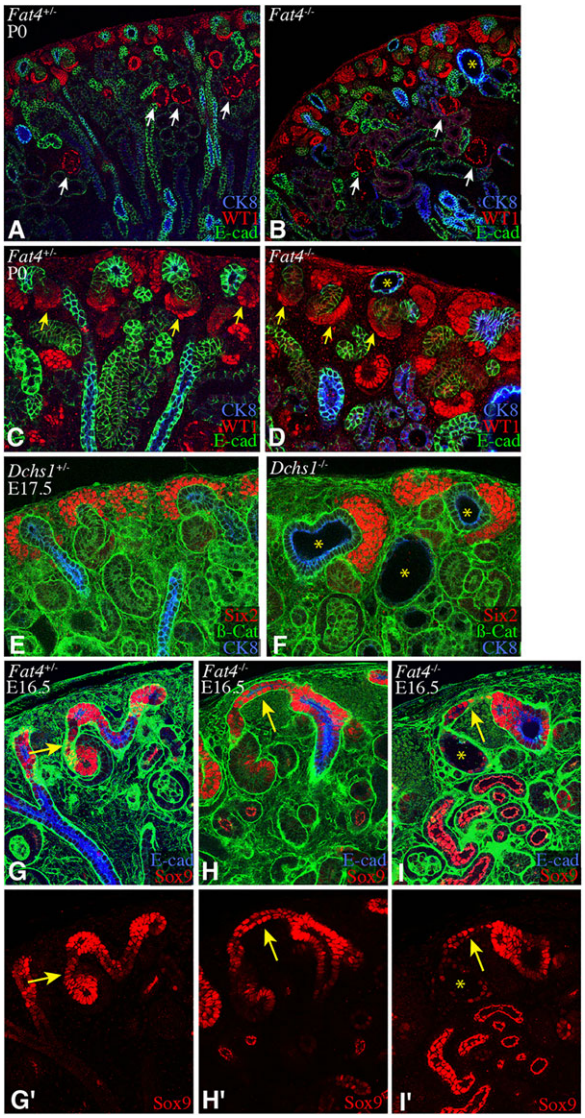

Fig. 4. Influence of *Dchs1* or *Fat4* mutation on early nephrogenesis. (A-I′) Confocal projections through sagittal vibratome sections of fetal or newborn kidneys. (A-D) Sibling control (A,C) and *Fat4* mutant (B,D) P0 kidneys at lower (A,B) and higher (C,D) magnification, stained for CK8 (blue), E-cad (green) and Wt1 (red). Wt1 is expressed in CM, and also within developing nephron in the lower part of RV, CB and SB (yellow arrows), and later in podocytes of Bowman's capsule (white arrows). (E,F) Sibling control (E) and *Dchs1* mutant (F) E16.5 kidneys, stained for CK8 (blue), β-cat (green) and Six2 (red), showing examples of cysts (asterisks) adjacent to CM. (G-I) Sibling control (G) and *Fat4* mutant (H,I) E16.5 kidneys, stained for E-cad (blue) and Sox9 (red). The green stain is a Six2 antisera with high non-specific background, used here as a counterstain. The connecting tubule and upper portion of SB express Sox9. Yellow arrows point to connecting tubules that in controls extend towards the medulla, whereas in mutants can extend parallel to the kidney surface, and terminate in cysts (I, asterisk) or abnormal SB (H). Panels marked by prime symbols show Sox9 stain alone.

the Wt1-expressing portion of the CB and SB is more variable, and often differs from that of wild type (Fig. 4C,D). Conditional deletion of *Dchs1* within CM also resulted in abnormal morphogenesis, including heterogeneity in the size and shape of the forming PA, RV and CB (supplementary material Fig. S3).

In addition to strong expression in UB tips, Sox9 is also expressed during early stages of nephrogenesis, when it is visible within connecting tubules and in proximal regions of the RV, CB or SB (Fig. 4G) (Reginensi et al., 2011). Using Sox9 as a marker, in wild-type kidneys Sox9-expressing tubules that extend away from the kidney surface can be observed connecting the UB to the SSB (Fig. 4G, arrow). By contrast, in *Dchs1* or *Fat4* mutant kidneys, the initial orientation of these connecting tubules is frequently (23/48 scored) abnormal, extending parallel to the surface of kidney (Fig. 4H,I). The ends of these Sox9-expressing tubules are often associated with cysts (Fig. 4I), which become even more evident at later stages (Fig. 4B,F). Accumulation of small cysts in P0 kidneys of *Dchs1* and *Fat4* mutants has been reported previously (Mao et al., 2011; Saburi et al., 2008); these cysts were identified in aquaporin 2-expressing (marks collecting duct and connecting tubule) and Tamm–Horsfall protein (THP; Umod – Mouse Genome Informatics)-expressing (marks nephron distal tubule and loop of Henle) tubules. We have extended cyst characterization here by identifying cysts in the outer (cortical) region associated with abnormal initiation of nephrogenesis; these cysts can express Sox9 or cytokeratin 8 (CK8, a marker of the UB; Krt8 – Mouse Genome Informatics) (Fig. 4B,D,F,I). We also note that we detect cysts not only at P0, but also at E17.5 and E16.5. This is potentially significant as it was proposed that tubule dilation could be ascribed to defects in oriented cell division (Saburi et al., 2008), but the existence of oriented cell divisions earlier than P0 has been controversial (Karner et al., 2009; Yu et al., 2009). Our observations emphasize that nephrogenesis occurs in *Dchs1* and *Fat4* mutants, but it is morphologically abnormal, and this abnormal nephron morphogenesis can be associated with cyst formation.

Examination of Yap and Taz in *Dchs1* and *Fat4* mutants

Das et al. (2013) concluded that the local increase in CM thickness in *Fat4* mutants stems from impaired differentiation of these nephron progenitor cells, and linked this impaired differentiation to activation of the Hippo pathway transcription factors Yap and Taz. This increased Yap/Taz activity was identified through increased nuclear localization of Yap in CM (Das et al., 2013). When we stained control kidneys, we observed a complex Yap distribution in the kidney, which appears to be consistent with previous studies (Das et al., 2013; Reginensi et al., 2013) and which includes cells with predominantly nuclear (which can be dispersed or concentrated in sub-nuclear foci), predominantly cytoplasmic, and mixed distributions of Yap (Fig. 5A; supplementary material Fig. S4A,C). The specificity of the antisera was confirmed by staining Yap mutant tissues (supplementary material Fig. S4D). However, when we examined Yap localization in either *Dchs1* or *Fat4* mutants, we were unable to detect an obvious difference in Yap localization between wild-type and mutant CM (Fig. 5B; supplementary material Fig. S4B). We are uncertain of the reason for this discrepancy with Das et al. (2013), but note that we examined Yap localization using both conventional antigen retrieval methods (Fig. 5A,B), as well as using the tyramide signal amplification (TSA) approach employed by Das et al. (2013) (supplementary material Fig. S4A,B).

To evaluate further the potential relationship between Fat4/Dchs1 signaling and Yap/Taz activity, we examined genetic interactions. In *Drosophila*, in which Fat regulates Yki activity, over-growth phenotypes of *fat* mutants are suppressed in *yki* heterozygotes (Reddy and Irvine, 2008). To assess whether a similar genetic interaction could be detected in murine kidneys, we compared $Dchs1^{-/-}$ or $Fat4^{-/-}$ kidneys with $Dchs1^{-/-}$ $Yap^{-/+}$ or $Fat4^{-/-}$ $Yap^{-/+}$ kidneys. However, neither overall kidney morphology nor the expansion of CM was visibly altered by loss of one copy of *Yap* (Fig. 5C-E; supplementary material Fig. S4E,F). Homozygous

Development (2015) 142, 2574-2585 doi:10.1242/dev.122630

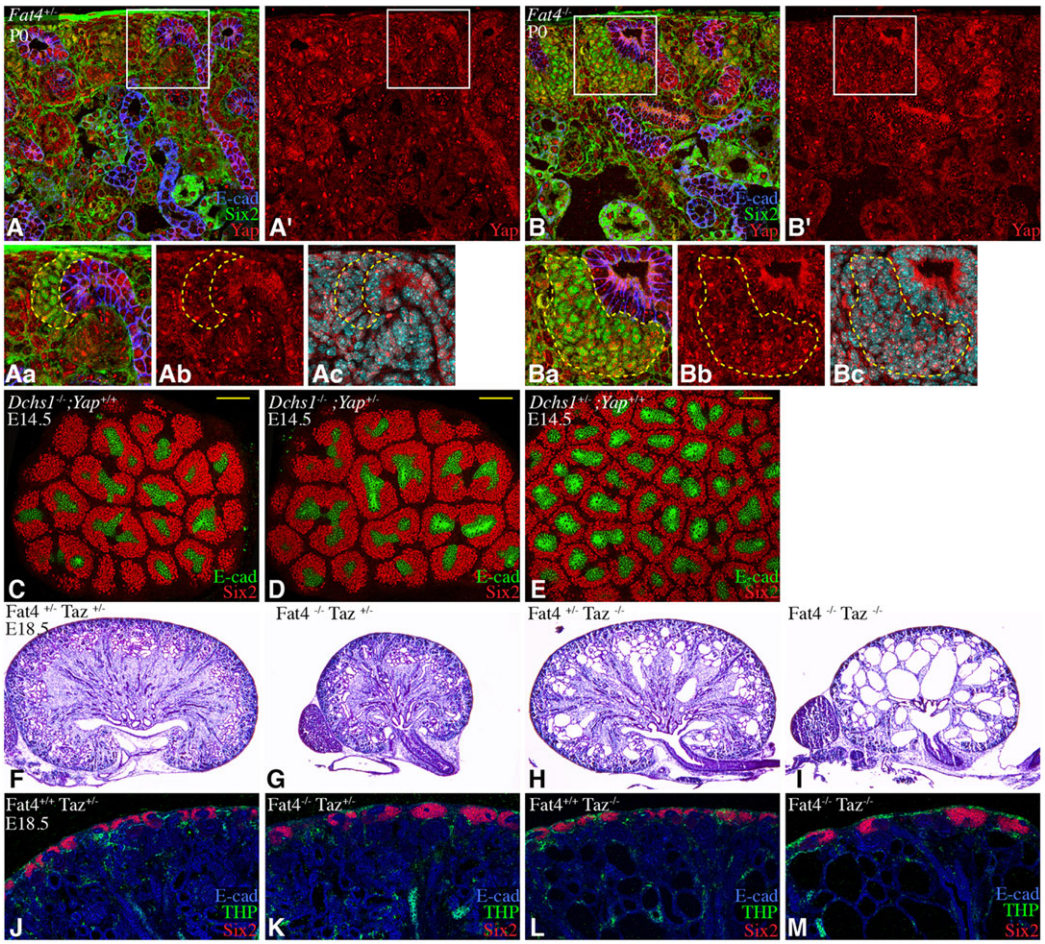

Fig. 5. Lack of interaction of *Dchs1* or *Fat4* with Yap and Taz. (A,B) Confocal images of sagittal sections, stained after antigen retrieval for Yap (red), Six2 (green), E-cad (blue) and DNA (cyan; Ac, Bc). The Six2 antisera used here has high non-specific background, but Six2-specific staining is nuclear. The boxed regions are shown at high magnification below (panels labeled a-c). A′, B′, Ab and Bb show Yap staining alone. Dashed yellow line outlines CM, which shows similar levels of heterogeneous Yap nuclear stain in wild type and mutants. (C-E) Surface sections of E14.5 *Dchs1*$^{-/-}$ *Yap*$^{+/+}$ (C), *Dchs1*$^{-/-}$ *Yap*$^{+/-}$ (D) and *Dchs1*$^{+/-}$ *Yap*$^{+/+}$ (E) sibling kidneys stained for Six2 (red) to reveal CM, and E-cad (green, expressed in UB). Scale bars: 100 µm. (F-I) Hematoxylin & Eosin-stained sections of *Fat4*$^{+/-}$ *Taz*$^{+/-}$ (F), *Fat4*$^{-/-}$ *Taz*$^{+/-}$ (G), *Fat4*$^{+/-}$ *Taz*$^{-/-}$ (H) and *Fat4*$^{-/-}$ *Taz*$^{-/-}$ (I) sibling E18.5 kidneys. (J-M) Confocal sections of *Fat4*$^{+/+}$ *Taz*$^{+/-}$ (J), *Fat4*$^{-/-}$ *Taz*$^{+/-}$ (K), *Fat4*$^{+/+}$ *Taz*$^{-/-}$ (L) and *Fat4*$^{-/-}$ *Taz*$^{-/-}$ (M) sibling kidneys, stained for Six2 (red), THP (green) and E-cad (blue).

Yap mutants die at E8.5, but homozygous *Taz* mutants can survive. However, mutation of *Taz* did not suppress *Fat4* kidney phenotypes, including smaller kidneys, reduced branching, and local expansion of CM (Fig. 5F-M; supplementary material Fig. S4G). Instead, we found that *Taz* mutants, which have a cystic kidney phenotype on their own (Hossain et al., 2007; Makita et al., 2008; Tian et al., 2007), and *Fat4* mutants, exhibit an enhanced cyst phenotype, such that *Fat4 Taz* double-mutant kidneys were almost entirely filled with large cysts (Fig. 5F-I; supplementary material Fig. S4G). Genetic enhancement between *Fat4* and *Taz* is also reflected in the fact that although we could readily obtain P0 *Fat4* or *Taz* single mutants, *Fat4 Taz* double mutants did not survive past E18.5. Thus, although earlier studies have revealed that Yap and Taz do play essential roles in kidney development (Das et al., 2013; Hossain et al., 2007; Makita et al., 2008; Reginensi et al., 2013; Tian et al., 2007), we did not obtain evidence supporting a role for Dchs1/Fat4 signaling in repression of Yap/Taz activity in CM.

Patterned expression of Dchs1 in cap mesenchyme

The determination that Dchs1 functions specifically within CM, and the implication that it participates in or influences signaling between stroma and CM, prompted us to examine its localization in greater detail. Close examination of Dchs1 protein in E14.5 kidneys revealed that it is not uniformly expressed in mesenchymal cells. Instead, its expression appears strongest along the outer edge of the CM, where CM cells abut stromal cells (Fig. 1B; Fig. 6). As Dchs1 is expressed in both stroma and CM, and indeed appears more strongly expressed in stroma, antibody staining in wild-type kidneys could not determine which cells are responsible for the strong Dchs1 protein staining near the CM-stromal interface. Thus, we conducted Dchs1 antibody staining on kidneys with conditional deletion of *Dchs1* in either of these cell populations. Conditional deletion of *Dchs1* using *Six2-Cre* led to absence of detectable Dchs1 staining in CM cells, with moderate expression remaining visible in stromal cells (Fig. 6B,D,F). Notably, the normal peak of Dchs1 staining at the stromal-mesenchymal interface was not observed. Conversely, when *Dchs1* was deleted specifically from stromal cells using *Foxd1-Cre*, a peak of Dchs1 expression at the stromal-mesenchymal interface remained visible (Fig. 6H,J,L). This peak of expression does not completely surround CM, but rather appears at discrete locations within a thin focal plane. This accumulation of Dchs1 protein reveals that Dchs1 expressed by CM cells can accumulate at high levels where they contact stromal cells. As Dchs1 in these same

Development (2015) 142, 2574-2585 doi:10.1242/dev.122630

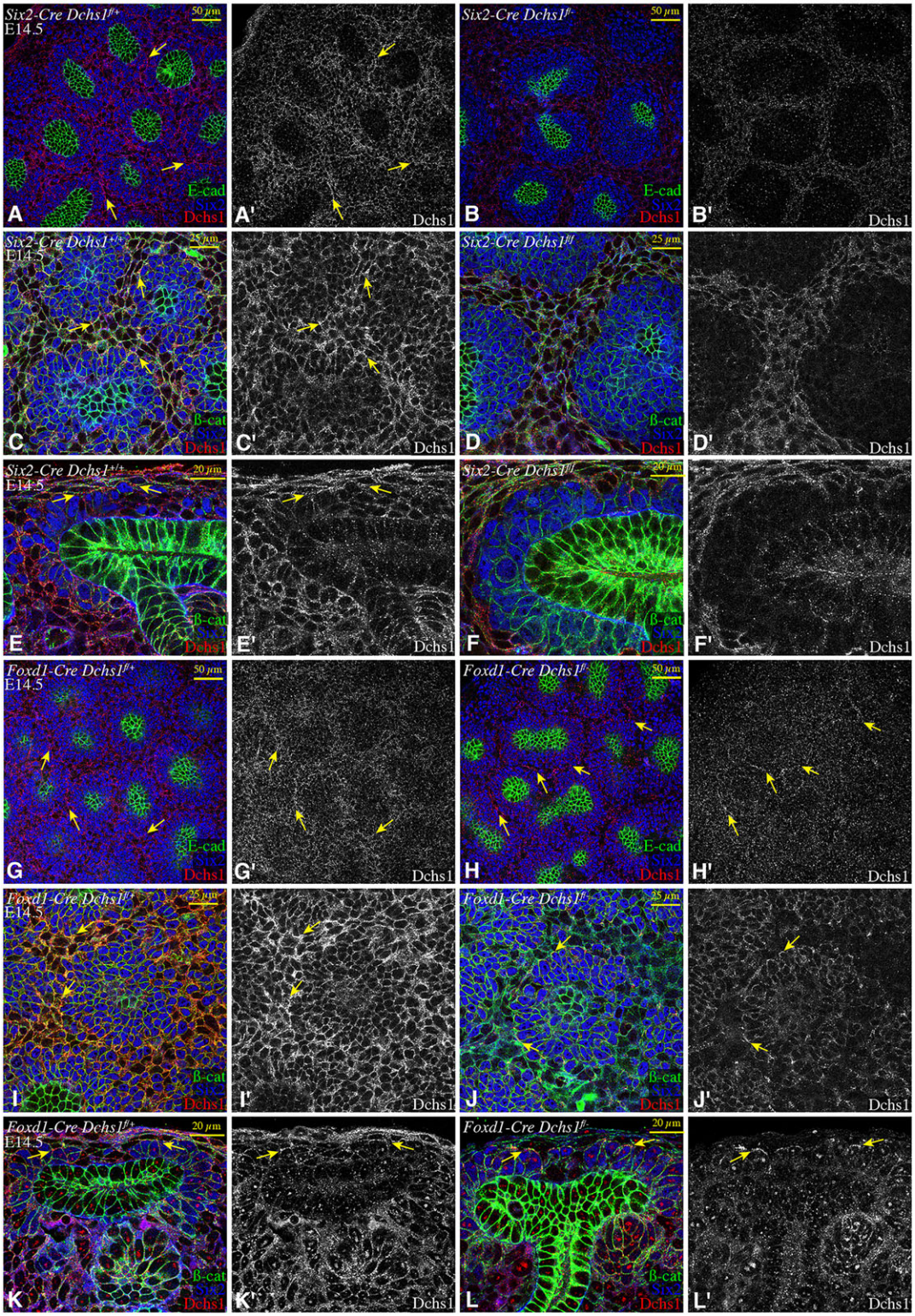

Fig. 6. Localization of Dchs1 at the CM-stroma interface. Confocal sections through E14.5 kidneys stained for Dchs1 (red/white), Six2 (blue), and E-cad or β-cat (green). Panels marked by prime symbols show Dchs1 stain only of the image to the left. Yellow arrows highlight examples of Dchs1 protein at the CM-stromal interface. Scale bar measurements are indicated. (A-D) Kidney surface sections of control (A,C) and conditional deletion of *Dchs1* in Six2-expressing cells (B,D). (E,F) Sagittal sections of control (E) and conditional deletion of *Dchs1* in Six2-expressing cells (F). (G-J) Kidney surface sections of control (G,I) and conditional deletion of *Dchs1* in Foxd1-expressing cells (H,J). (K,L) Sagittal sections of control (K) and conditional deletion of *Dchs1* in Foxd1-expressing cells (L).

cells does not accumulate to similar levels on cell membranes not in contact with stromal cells, these observations identify a molecular polarization of these outer CM cells. Polarization of Ds protein localization has been observed in *Drosophila* (Ambegaonkar et al., 2012; Bosveld et al., 2012; Brittle et al., 2012) and is thought to be crucial for establishment of PCP by the Ds/Fat pathway, but

Development (2015) 142, 2574-2585 doi:10.1242/dev.122630

polarization of Dchs1 in vertebrates has not previously been reported.

As CM condenses into the RV, Dchs1 protein accumulates apically (supplementary material Fig. S3C,E). However, as E-cad also concentrates apically in these cells, this might simply reflect the emerging apical-basal polarity of these cells, rather than a specific role for Dchs1 in RV formation.

DISCUSSION

Metanephric kidney development requires coordinated signaling among stroma, CM and UB. Our analysis of Dchs1 establishes that it plays an essential role in signaling between the stroma and CM, and that it functions specifically within CM to promote the differentiation and morphogenesis of these nephron progenitors. The importance of stroma-to-CM signaling in kidney development was first revealed by the mutant phenotypes of genes expressed in stromal cells, and by analysis of stroma-less kidneys (Das et al., 2013; Hatini et al., 1996; Hum et al., 2014; Levinson et al., 2005; Paroly et al., 2013). Fat4 was implicated in this process because of the similarity of *Fat4* mutant phenotypes to the stroma-less phenotype (Das et al., 2013). Our analysis of *Dchs1* and *Fat4* reveals that they have similar mutant phenotypes throughout the kidney, resembling those of stroma-less kidneys (Das et al., 2013; Hum et al., 2014). Thus, we infer that Fat4/Dchs1 signaling is an essential mediator of stromal-to-CM signaling. The direct participation of Dchs1 in stromal-CM signaling is further supported by the detection of Dchs1 protein accumulation at the stroma-CM interface. We note that Bagherie-Lachidan et al. (2015) report a contribution of *Dchs2* to kidney development, which is revealed by the observation that the *Dchs1* kidney phenotype is slightly weaker than the *Fat4* kidney phenotype, whereas the *Dchs1 Dchs2* double mutant phenotype is equivalent to *Fat4*.

Tissue-specific conditional deletion reveals that Dchs1 acts specifically within CM to influence kidney development. Through conditional deletion of Fat4, Bagherie-Lachidan et al. (2015) determined that Fat4 acts specifically within Foxd1-expressing cortical stroma. These genetic results imply that they act as signaling partners to effect signaling between stroma and CM, with Fat4 in stromal cells communicating with Dchs1 in CM. As *Drosophila* homologs of Dchs1 and Fat4 (Ds and Fat) bind each other (Matis and Axelrod, 2013), it is likely that this Fat4-Dchs1-dependent signaling is also mediated by direct binding, and this suggestion is supported by the accumulation of Dchs1 in CM at sites of contact with stroma. Another distinctive feature of Fat4/Dchs1 signaling revealed by our studies is its deployment in communication between distinct cell layers composed of different cell types. In *Drosophila*, in which Ds/Fat signaling is best known for its role in helping cells interpret and respond to molecular gradients (Matis and Axelrod, 2013; Reddy and Irvine, 2008), Ds/Fat signaling occurs among neighboring cells within an epithelial monolayer. In the mammalian kidney, by contrast, we report here that Fat4/Dchs1 signaling participates in inductive signaling between neighboring mesenchymal cell populations.

Several possible mechanisms by which Fat4/Dchs1 signaling modulates nephrogenesis can be considered based on our current understanding of these genes and their phenotypes (Fig. 7). First, Fat4 and Dchs1 might act as ligand and receptor, respectively, for an intercellular signaling pathway that controls a transcriptional program within CM necessary for nephron morphogenesis (Fig. 7A). Indeed, Das et al. (2013) proposed that Fat4-dependent signaling from stromal cells inhibits CM differentiation by activating the Hippo pathway transcriptional co-activators Yap and Taz. However, neither we nor Bagherie-Lachidan et al. (2015) could detect changes in Yap localization in *Fat4* or *Dchs1* mutants that would be consistent with increased Yap activation, nor did we find support for this hypothesis in our examinations of genetic interactions between *Yap* and *Fat4* or *Dchs1*, or between *Taz* and *Fat4*. Additionally, we note that although Ds/Fat signaling influences the activity of the Yap homolog Yki in *Drosophila*, the manner in which it regulates Yki differs from the regulation of Yap reported by Das et al. (2013). In the best-studied *Drosophila* Fat/Hippo pathway, Ds acts as a ligand and Fat acts as a receptor, such that if this pathway were operating we would have expected Yap activation within stromal cells in *Fat4* or *Dchs1* mutants, rather than within CM. There is also some evidence in *Drosophila* for a reverse, Fat-to-Ds signal, but this reverse signal appears to activate rather than inhibit Yki (Degoutin et al., 2013), such that if this pathway were operating we would have expected decreased, rather than increased, Yap activity in *Fat4* or *Dchs1* mutants. These observations, together with the absence of the key Fat/Hippo pathway transducer Dachs in vertebrates (Bossuyt et al., 2014), and the inability of Fat4 to provide Hippo pathway activity in transgenic *Drosophila* (Pan et al., 2013), emphasize that if there is transcriptional pathway activated by Fat4/Dchs1 signaling in the kidney, it must involve a mechanism unrelated to any so far described in *Drosophila*.

A second potential class of models for how Fat4 and Dchs1 influence nephrogenesis invokes signaling from Dchs1 in CM to Fat4 in stroma to induce a transcriptional program that influences stromal cells, including production of additional signals that feedback and influence the CM and/or UB (Fig. 7B). Although this possibility cannot be excluded, we do not favor it, as it would require the existence of additional, as yet unidentified, stromal signals. Known stromal genes that influence kidney development (Foxd1, Ecm1, Dcn) were not significantly affected in *Fat4* mutants. Conversely, the hypothesis that Fat4 in stroma signals to Dchs1 in CM does not require invoking additional, as yet unidentified, signals to explain why ablation of stroma phenocopies *Fat4* and *Dchs1* mutants.

In another class of models, the altered behavior of CM cells and abnormal nephrogenesis could stem from disturbances in cell polarity rather than transcriptional targets of Fat4/Dchs1 signaling (Fig. 7C). In contrast to the lack of evidence for conservation of the connection to Hippo signaling, the influence of Dchs1 and Fat4 on PCP is clearly conserved in mammals (Mao et al., 2011; Pan et al., 2013; Saburi et al., 2008; Zakaria et al., 2014). Our studies have provided further support for this conservation by using genetic mosaics to show that Dchs1 protein can be molecularly polarized in vertebrate cells. In *Drosophila*, Ds protein localization is polarized by differential expression of Fat in neighboring cells, and this polarization is thought to be crucial for the establishment of PCP (Matis and Axelrod, 2013). Polarization of cellular organization could modulate the responsiveness of CM to additional signals from their neighbors, and/or their ability to signal to other cells. For example, in the *Drosophila* leg, PCP signaling modulates Notch signaling through effects on Notch receptor endocytosis (Capilla et al., 2012). Interestingly, Notch signaling also plays essential roles in nephrogenesis, as *Notch2* mutant cells are unable to form proximal tubules (Cheng et al., 2007). PCP is also well known to influence polarized cell behaviors, including cell migration and cell intercalation, which might be reflected in the mispositioning and misorientation of developing nephron structures that we observe.

In analyzing stroma-less kidneys, Das et al. (2013) reported a frequent block in differentiation, which they attributed to increased activation of Yap and Taz. However, Hum et al. (2014) emphasized

Development (2015) 142, 2574-2585 doi:10.1242/dev.122630

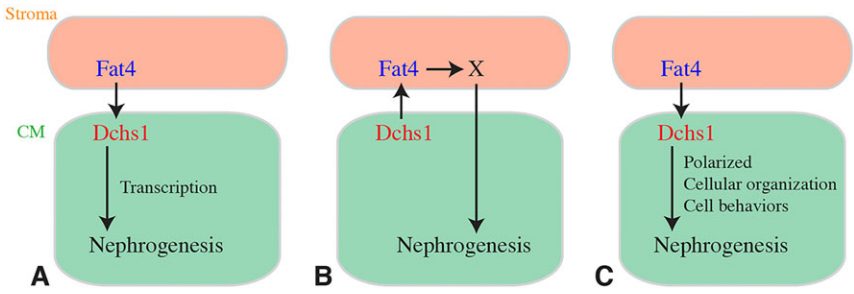

Fig. 7. Potential mechanisms for influence of Fat4/Dchs1 signaling on nephrogenesis. Schematic of signaling between stromal cells (orange) and CM (green). (A) Fat4 could act as a ligand for Dchs1 to directly activate a transcriptional program in CM required for normal nephrogenesis. (B) Dchs1 could act as a ligand for Fat4 to activate expression of factors (X) in stroma that signal back to CM to direct normal nephrogenesis. (C) Fat4/Dchs1 signaling could establish a polarization of adjacent CM that is essential for nephrogenesis, because it influences responsiveness to additional signals, and/or polarizes cell behaviors. See text for details.

the mispositioning of differentiated nephron structures, while reporting that differentiation still occurs. In characterizing *Dchs1* and *Fat4* mutants, we and Bagherie-Lachidan et al. (2015) frequently observe differentiated nephron structures (e.g. Wt1-expressing podocytes), and also clearly observe cells undergoing early stages of nephrogenesis. However, the location and arrangement of these cells is frequently abnormal, as evidenced by the abnormal location and arrangement of Sox9-expressing cells in the upper SB and Wt1-expressing cells in the lower SB, and the disorganization of forming RV. In some cases, cysts form in cortical regions from cells that express markers of the UB or connecting tubules, possibly because defects in nephrogenesis have left these as blind sacs.

Dchs1 or *Fat4* mutations also impair UB growth and branching, even though they are not genetically required in the UB. It could be that Dchs1/Fat4 signaling promotes the production of an as yet unidentified signal from the CM or stroma that represses UB tip cell fate, resulting within mutants in both an increased exposure of CM to UB tip cell signals, and decreased UB branching. However, we favor what we consider to be a simpler hypothesis, as it does not invoke additional, as yet unidentified signals: the Dchs1-Fat4 phenotype in the UB could be accounted for by proposing that the lack of Dchs1 within the CM (or lack of interaction with Fat4) leads to a local expansion of CM, which, by virtue of the known role of CM in maintaining UB tip cell fate, then impairs UB morphogenesis. Consistent with these hypotheses, we observed an expansion of tip cell markers in mutants; a similar expansion of tip markers was recently reported in stroma-less kidneys (Hum et al., 2014). Moreover, differences in contact between CM and UB in mutants are visible as early as E11.5, around the time that branching defects first appear in *Fat4* or *Dchs1* mutants (Mao et al., 2011). These observations emphasize that normal kidney branching and growth requires a delicate balance between tip and trunk cell fates within the UB. Moreover, the appearance of reduced UB branching as a prominent phenotypic consequence of disturbed stromal-CM signaling highlights the intricate coordination of signaling interactions among tissue layers required for kidney morphogenesis.

MATERIALS AND METHODS

Mice

Gene-targeted mutations in *Fat4* and *Dchs1*, *Vangl2*^{Lp}, and Cre-expressing lines *Hoxb7-Cre*, *Six2-EGFP/Cre* and *Foxd1-GFP/Cre*, have been described previously (Copp et al., 1994; Humphreys et al., 2010; Kobayashi et al., 2008; Mao et al., 2011; Saburi et al., 2008; Yu et al., 2002). Yap heterozygous mice were generated by converting a published conditional allele (Zhang et al., 2010) with *Tg(Sox2-Cre)1Amc/J* (Jackson Laboratory). *Taz* (*Wwtr1*) mutant mice, *Cited1-tagRFP* and conditional *Rosa26-lacZ* mice were obtained from the Jackson Laboratory. Animals were housed in an Institutional Animal Care and Use Committee (IACUC)-approved facility using IACUC-approved protocols. Genotyping was performed as described previously (Mao et al., 2011).

Histology and imaging

E14.0 or older whole kidneys were cut longitudinally into halves with razor blades before antibody staining. For vibratome sections, kidneys were first mounted in 3% low gelling temperature agarose (Sigma, A0701-25G), and cut at 100 µm thickness, and mounted with 100-µm glass beads as spacers to prevent tissue compression. Antibody staining of whole kidneys or sections was performed as described previously (Mao et al., 2011), using the following primary antibodies: goat anti-β-catenin (AF1329, R&D Systems; 1:100), goat anti-E-cadherin (AF748, R&D Systems; 1:400), rabbit anti-Six2 (11562-1-AP, Proteintech; 1:300), mouse anti-Six2 (H00010736-M01, Abnova; 1:400), rabbit anti-Wt1 (SC-192, Santa Cruz; 1:50), rabbit anti-Sox9 (AB5535, Millipore; 1:400), chicken anti-GFP (GFP-1020, Aves lab; 1:1000), rat anti-CK8 (Troma-I, Developmental Studies Hybridoma Bank, Troma-I; 1:200), rat anti-Fat4 (gift of T. Tanoue) (Ishiuchi et al., 2009), rabbit anti-tagRFP (AB233, Evrogen; 1:800) and mouse anti-phospho-Histone H3 (9706, Cell Signaling; 1:400). For *Dolichos biflorus* agglutinin (DBA) staining, kidneys were fixed with methanol at −20°C, and stained using DBA-biotin (L6533, Sigma; 1:300). For tyramide signal amplification (TSA), slides were treated first for antigen retrieval, and then incubated with primary antibodies, including rabbit anti-Yap1 (4912S, Cell Signaling; 1:400). Slides were then incubated with appropriate fluorescent secondary antibodies (donkey anti-mouse 488, Life Technologies, A21202; and donkey anti-goat 647, Jackson ImmunoResearch, 705-495-147) plus anti-rabbit IgG-biotin (donkey anti-rabbit, Jackson ImmunoResearch, 111-065-152, Jackson ImmunoResearch) to detect Yap1 antibody, and biotin signals were amplified using HRP-streptavidin and Alexa Fluor 546 tyramide (TSA kit, T20933, Life Technologies). Secondary antibodies were from Jackson ImmunoResearch, and stained kidneys were imaged on a Leica SP5 confocal microscope.

For X-gal staining, P0 kidneys were fixed in 4% paraformaldehyde for 4 h at 4°C, then frozen, and sections were cut at 12 µm thickness. Slides were washed twice with PBS plus 2 mM $MgCl_2$, 0.01% deoxycholate and 0.02% NP-40, and incubated in freshly made and filtered staining solution {2 mM $MgCl_2$, 5 mM potassium ferrocyanide [$K_4Fe(CN)_6$-$3H_20$] and 5 mM potassium ferricyanide [$K_3Fe(CN)_6$], 1 mg/ml X-gal} for 17 h at 37°C under darkness, washed again with PBS, and counter-stained with Nuclear Fast Red.

Quantitative PCR

Total RNAs were extracted from E14.5 *Fat4* wild-type and mutant kidneys using the Life Technologies PARIS kit. RNA extraction was performed on ten wild-type and 22 mutant kidneys from four litters. cDNAs were made using the SuperScript VILO cDNA Synthesis kit. Quantitative PCR was performed in a Life Technologies StepOnePlus, using SYBR Select Master Mix. Primers are listed in the supplementary material.

Measurements

For measuring ureteric tip areas, Sox9-stained tips were measured using Leica LAS AF software. Because of the curved nature of kidney surface, only tips in the center area of the scanned field were measured, and the confocal *z* section at which the tip area was the biggest was used to determine tip area. Bud tips were counted manually from 3D confocal stacks. Statistical tests were performed using Graphpad Prism software. For measuring the total volume of Cited1-tagRFP-positive cells, confocal stacks were analyzed using Volocity (PerkinElmer) software.

Acknowledgements
We thank E. Kirichenko for assistance with genotyping; D. Pan, H. McNeill, A. McMahon, T. Tanoue and J. Yu for reagents; H. McNeill for communication of unpublished results; and F. Costantini and J. Davies for helpful advice.

Competing interests
The authors declare no competing or financial interests.

Author contributions
Y.M designed, performed and analyzed experiments and wrote the manuscript. P.F.-W. and K.D.I. supervised research, designed and analyzed experiments, and wrote the manuscript.

Funding
This research was funded by the Biotechnology and Biological Sciences Research Council (BBSRC) [BB/K001671/1 to P.F.-W.]; and the Howard Hughes Medical Institute (K.D.I.). Deposited in PMC for release after 6 months.

Supplementary material
Supplementary material available online at
http://dev.biologists.org/lookup/suppl/doi:10.1242/dev.122630/-/DC1

References

Ambegaonkar, A. A., Pan, G., Mani, M., Feng, Y. and Irvine, K. D. (2012). Propagation of Dachsous-fat planar cell polarity. *Curr. Biol.* **22**, 1302-1308.
Bagherie-Lachidan, M., Reginensi, A., Zaveri, H. P., Scott, D. A., Helmbacher, F. and McNeill, H. (2015). Stromal Fat4 acts non-autonomously with Dchs1/2 to restrict the nephron progenitor pool. *Development* **142**, 2564-2573.
Bossuyt, W., Chen, C.-L., Chen, Q., Sudol, M., McNeill, H., Pan, D., Kopp, A. and Halder, G. (2014). An evolutionary shift in the regulation of the Hippo pathway between mice and flies. *Oncogene* **33**, 1218-1228.
Bosveld, F., Bonnet, I., Guirao, B., Tlili, S., Wang, Z., Petitalot, A., Marchand, R., Bardet, P.-L., Marcq, P., Graner, F. et al. (2012). Mechanical control of morphogenesis by Fat/Dachsous/Four-jointed planar cell polarity pathway. *Science* **336**, 724-727.
Brittle, A., Thomas, C. and Strutt, D. (2012). Planar polarity specification through asymmetric subcellular localization of fat and Dachsous. *Curr. Biol.* **22**, 907-914.
Capilla, A., Johnson, R., Daniels, M., Benavente, M., Bray, S. J. and Galindo, M. I. (2012). Planar cell polarity controls directional Notch signaling in the Drosophila leg. *Development* **139**, 2584-2593.
Cappello, S., Gray, M. J., Badouel, C., Lange, S., Einsiedler, M., Srour, M., Chitayat, D., Hamdan, F. F., Jenkins, Z. A., Morgan, T. et al. (2013). Mutations in genes encoding the cadherin receptor-ligand pair DCHS1 and FAT4 disrupt cerebral cortical development. *Nat. Genet.* **45**, 1300-1308.
Cheng, H.-T., Kim, M. T., Valerius, M. T., Surendran, K., Schuster-Gossler, K., Gossler, A., McMahon, A. P. and Kopan, R. (2007). Notch2, but not Notch1, is required for proximal fate acquisition in the mammalian nephron. *Development* **134**, 801-811.
Copp, A. J., Checiu, I. and Henson, J. N. (1994). Developmental basis of severe neural tube defects in the loop-tail (Lp) mutant mouse: use of microsatellite DNA markers to identify embryonic genotype. *Dev. Biol.* **165**, 20-29.
Costantini, F. and Kopan, R. (2010). Patterning a complex organ: branching morphogenesis and nephron segmentation in kidney development. *Dev. Cell* **18**, 698-712.
Das, A., Tanigawa, S., Karner, C. M., Xin, M., Lum, L., Chen, C., Olson, E. N., Perantoni, A. O. and Carroll, T. J. (2013). Stromal–epithelial crosstalk regulates kidney progenitor cell differentiation. *Nat. Cell Biol.* **15**, 1035-1044.
Degoutin, J. L., Milton, C. C., Yu, E., Tipping, M., Bosveld, F., Yang, L., Bellaïche, Y., Veraksa, A. and Harvey, K. F. (2013). Riquiqui and minibrain are regulators of the hippo pathway downstream of Dachsous. *Nat. Cell Biol.* **15**, 1176-1185.
Dressler, G. R. (2009). Advances in early kidney specification, development and patterning. *Development* **136**, 3863-3874.
Fetting, J. L., Guay, J. A., Karolak, M. J., Iozzo, R. V., Adams, D. C., Maridas, D. E., Brown, A. C. and Oxburgh, L. (2014). FOXD1 promotes nephron progenitor differentiation by repressing decorin in the embryonic kidney. *Development* **141**, 17-27.
Goodrich, L. V. and Strutt, D. (2011). Principles of planar polarity in animal development. *Development* **138**, 1877-1892.
Hatini, V., Huh, S. O., Herzlinger, D., Soares, V. C. and Lai, E. C. (1996). Essential role of stromal mesenchyme in kidney morphogenesis revealed by targeted disruption of Winged Helix transcription factor BF-2. *Genes Dev.* **10**, 1467-1478.
Hossain, Z., Ali, S. M., Ko, H. L., Xu, J., Ng, C. P., Guo, K., Qi, Z., Ponniah, S., Hong, W. and Hunziker, W. (2007). Glomerulocystic kidney disease in mice with a targeted inactivation of Wwtr1. *Proc. Natl. Acad. Sci. USA* **104**, 1631-1636.
Hum, S., Rymer, C., Schaefer, C., Bushnell, D. and Sims-Lucas, S. (2014). Ablation of the renal stroma defines its critical role in nephron progenitor and vasculature patterning. *PLoS ONE* **9**, e88400.
Humphreys, B. D., Lin, S.-L., Kobayashi, A., Hudson, T. E., Nowlin, B. T., Bonventre, J. V., Valerius, M. T., Mcmahon, A. P. and Duffield, J. S. (2010). Fate tracing reveals the pericyte and not epithelial origin of myofibroblasts in kidney fibrosis. *Am. J. Pathol.* **176**, 85-97.
Ishiuchi, T., Misaki, K., Yonemura, S., Takeichi, M. and Tanoue, T. (2009). Mammalian Fat and Dachsous cadherins regulate apical membrane organization in the embryonic cerebral cortex. *J. Cell Biol.* **185**, 959-967.
Karner, C. M., Chirumamilla, R., Aoki, S., Igarashi, P., Wallingford, J. B. and Carroll, T. J. (2009). Wnt9b signaling regulates planar cell polarity and kidney tubule morphogenesis. *Nat. Genet.* **41**, 793-799.
Kobayashi, A., Valerius, M. T., Mugford, J. W., Carroll, T. J., Self, M., Oliver, G. and Mcmahon, A. P. (2008). Six2 defines and regulates a multipotent self-renewing nephron progenitor population throughout mammalian kidney development. *Cell Stem Cell* **3**, 169-181.
Kopan, R., Chen, S. and Little, M. (2014). Nephron progenitor cells: shifting the balance of self-renewal and differentiation. *Curr. Top. Dev. Biol.* **107**, 293-331.
Levinson, R. S., Batourina, E., Choi, C., Vorontchikhina, M., Kitajewski, J. and Mendelsohn, C. L. (2005). Foxd1-dependent signals control cellularity in the renal capsule, a structure required for normal renal development. *Development* **132**, 529-539.
Makita, R., Uchijima, Y., Nishiyama, K., Amano, T., Chen, Q., Takeuchi, T., Mitani, A., Nagase, T., Yatomi, Y., Aburatani, H. et al. (2008). Multiple renal cysts, urinary concentration defects, and pulmonary emphysematous changes in mice lacking TAZ. *Am. J. Renal Physiol.* **294**, F542-F553.
Mansour, S., Swinkels, M., Terhal, P. A., Wilson, L. C., Rich, P., Van Maldergem, L., Zwijnenburg, P. J. G., Hall, C. M., Robertson, S. P. and Newbury-Ecob, R. (2012). Van Maldergem syndrome: further characterisation and evidence for neuronal migration abnormalities and autosomal recessive inheritance. *Eur. J. Hum. Genet.* **20**, 1024-1031.
Mao, Y., Mulvaney, J., Zakaria, S., Yu, T., Morgan, K. M., Allen, S., Basson, M. A., Francis-West, P. and Irvine, K. D. (2011). Characterization of a Dchs1 mutant mouse reveals requirements for Dchs1-Fat4 signaling during mammalian development. *Development* **138**, 947-957.
Matis, M. and Axelrod, J. D. (2013). Regulation of PCP by the Fat signaling pathway. *Genes Dev.* **27**, 2207-2220.
Oliver, G., Wehr, R., Jenkins, N. A., Copeland, N. G., Cheyette, B. N., Hartenstein, V., Zipursky, S. L. and Gruss, P. (1995). Homeobox genes and connective tissue patterning. *Development* **121**, 693-705.
Pan, D. (2010). The hippo signaling pathway in development and cancer. *Dev. Cell* **19**, 491-505.
Pan, G., Feng, Y., Ambegaonkar, A. A., Sun, G., Huff, M., Rauskolb, C. and Irvine, K. D. (2013). Signal transduction by the Fat cytoplasmic domain. *Development* **140**, 831-842.
Paroly, S. S., Wang, F., Spraggon, L., Merregaert, J., Batourina, E., Tycko, B., Schmidt-Ott, K. M., Grimmond, S., Little, M. and Mendelsohn, C. (2013). Stromal protein Ecm1 regulates ureteric bud patterning and branching. *PLoS ONE* **8**, e84155.
Reddy, B. V. V. G. and Irvine, K. D. (2008). The Fat and Warts signaling pathways: new insights into their regulation, mechanism and conservation. *Development* **135**, 2827-2838.
Reginensi, A., Clarkson, M., Neirijnck, Y., Lu, B., Ohyama, T., Groves, A. K., Sock, E., Wegner, M., Costantini, F., Chaboissier, M.-C. et al. (2011). SOX9 controls epithelial branching by activating RET effector genes during kidney development. *Hum. Mol. Genet.* **20**, 1143-1153.
Reginensi, A., Scott, R. P., Gregorieff, A., Bagherie-Lachidan, M., Chung, C., Lim, D.-S., Pawson, T., Wrana, J. and McNeill, H. (2013). Yap- and Cdc42-dependent nephrogenesis and morphogenesis during mouse kidney development. *PLoS Genet.* **9**, e1003380.
Saburi, S., Hester, I., Fischer, E., Pontoglio, M., Eremina, V., Gessler, M., Quaggin, S. E., Harrison, R., Mount, R. and McNeill, H. (2008). Loss of Fat4 disrupts PCP signaling and oriented cell division and leads to cystic kidney disease. *Nat. Genet.* **40**, 1010-1015.
Saburi, S., Hester, I., Goodrich, L. and McNeill, H. (2012). Functional interactions between Fat family cadherins in tissue morphogenesis and planar polarity. *Development* **139**, 1806-1820.
Soriano, P. (1999). Generalized lacZ expression with the ROSA26 Cre reporter strain. *Nat. Genet.* **21**, 70-71.
Staley, B. K. and Irvine, K. D. (2012). Hippo signaling in Drosophila: recent advances and insights. *Dev. Dyn.* **241**, 3-15.
Thomas, C. and Strutt, D. (2012). The roles of the cadherins Fat and Dachsous in planar polarity specification in Drosophila. *Dev. Dyn.* **241**, 27-39.
Tian, Y., Kolb, R., Hong, J.-H., Carroll, J., Li, D., You, J., Bronson, R., Yaffe, M. B., Zhou, J. and Benjamin, T. (2007). TAZ promotes PC2 degradation through a SCFbeta-Trcp E3 ligase complex. *Mol. Cell. Biol.* **27**, 6383-6395.
Wansleeben, C. and Meijlink, F. (2011). The planar cell polarity pathway in vertebrate development. *Dev. Dyn.* **240**, 616-626.

Development (2015) 142, 2574-2585 doi:10.1242/dev.122630

Yates, L. L., Papakrivopoulou, J., Long, D. A., Goggolidou, P., Connolly, J. O., Woolf, A. S. and Dean, C. H. (2010). The planar cell polarity gene Vangl2 is required for mammalian kidney-branching morphogenesis and glomerular maturation. *Hum. Mol. Genet.* **19**, 4663-4676.

Yu, J., Carroll, T. J. and Mcmahon, A. P. (2002). Sonic hedgehog regulates proliferation and differentiation of mesenchymal cells in the mouse metanephric kidney. *Development* **129**, 5301-5312.

Yu, J., Carroll, T. J., Rajagopal, J., Kobayashi, A., Ren, Q. and Mcmahon, A. P. (2009). A Wnt7b-dependent pathway regulates the orientation of epithelial cell division and establishes the cortico-medullary axis of the mammalian kidney. *Development* **136**, 161-171.

Zakaria, S., Mao, Y., Kuta, A., Ferreira de Sousa, C., Gaufo, G. O., McNeill, H., Hindges, R., Guthrie, S., Irvine, K. D. and Francis-West, P. H. (2014). Regulation of neuronal migration by dchs1-fat4 planar cell polarity. *Curr. Biol.* **24**, 1620-1627.

Zhang, N., Bai, H., David, K. K., Dong, J., Zheng, Y., Cai, J., Giovannini, M., Liu, P., Anders, R. A. and Pan, D. (2010). The Merlin/NF2 tumor suppressor functions through the YAP oncoprotein to regulate tissue homeostasis in mammals. *Dev. Cell* **19**, 27-38.

Supplemental Material For Mao et al, A Fat4-Dchs1 signal between stromal and cap mesenchyme cells influences nephrogenesis and ureteric bud branching

Supplementary Methods

Primer sequences:

GapdhF AGGTCGGTGTGAACGGATTTG

GapdhR TGTAGACCATGTAGTTGAGGTCA

six2F: CACCTCCACAAGAATGAAAGCG

six2R: CTCCGCCTCGATGTAGTGC

wnt7bF: TTTGGCGTCCTCTACGTGAAG

wnt7bR: CCCCGATCACAATGATGGCA

retF: GCATGTCAGACCCGAACTGG

retR: CGCTGAGGGTGAAACCATCC

sox9F: GAGCCGGATCTGAAGAaGGA

sox9R: GCTTGACGTGTGGCTTGTTC

E-CadF: CAGGTCTCCTCATGGCTTTGC

E-cadR: CTTCCGAAAAGAAGGCTGTCC

Ecm1F: GGGACCGTATCCAGAGCAG

Ecm1R: GCTGGTCTGAAGCCTTGAAG

DcnF: TCTTGGGCTGGACCATTTGAA

DcnR: CATCGGTAGGGGCACATAGA

Primers sequences were designed using http://pga.mgh.harvard.edu/primerbank/.

Supplementary Figures

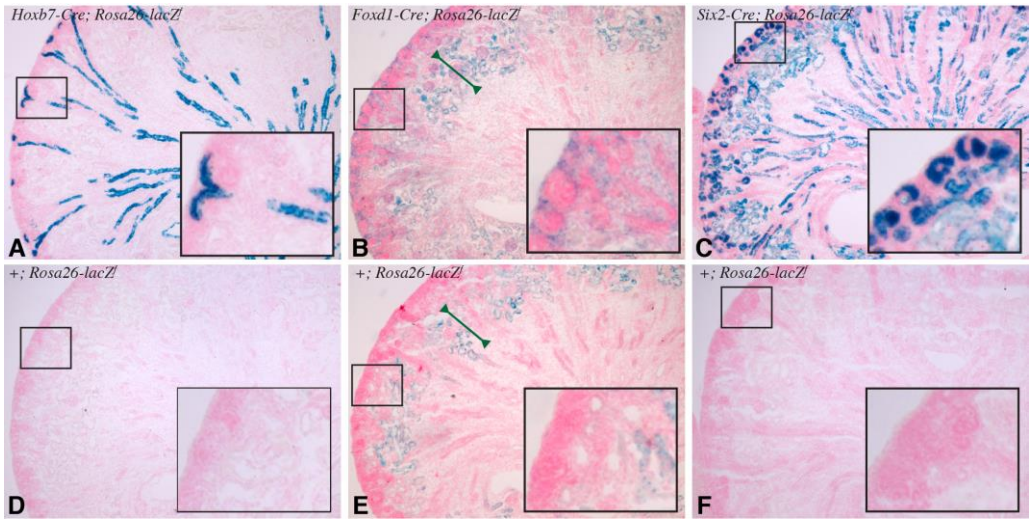

Figure S1. Confirmation of tissue-specific Cre activity

Sections of Newborn (P0) mouse kidneys subject to histochemical staining for ß-galactosidase activity expressed from a conditional Rosa26-lacZ allele. A) Hoxb7-Cre B) Foxd1-Cre C) Six2-Cre. D-F) show sibling controls that lack Cre-expressing alleles. Insets show higher magnification of the boxed region encompassing uteric distal tip and nephrogenic precursors. Sections were counterstained with nuclear Fast Red.

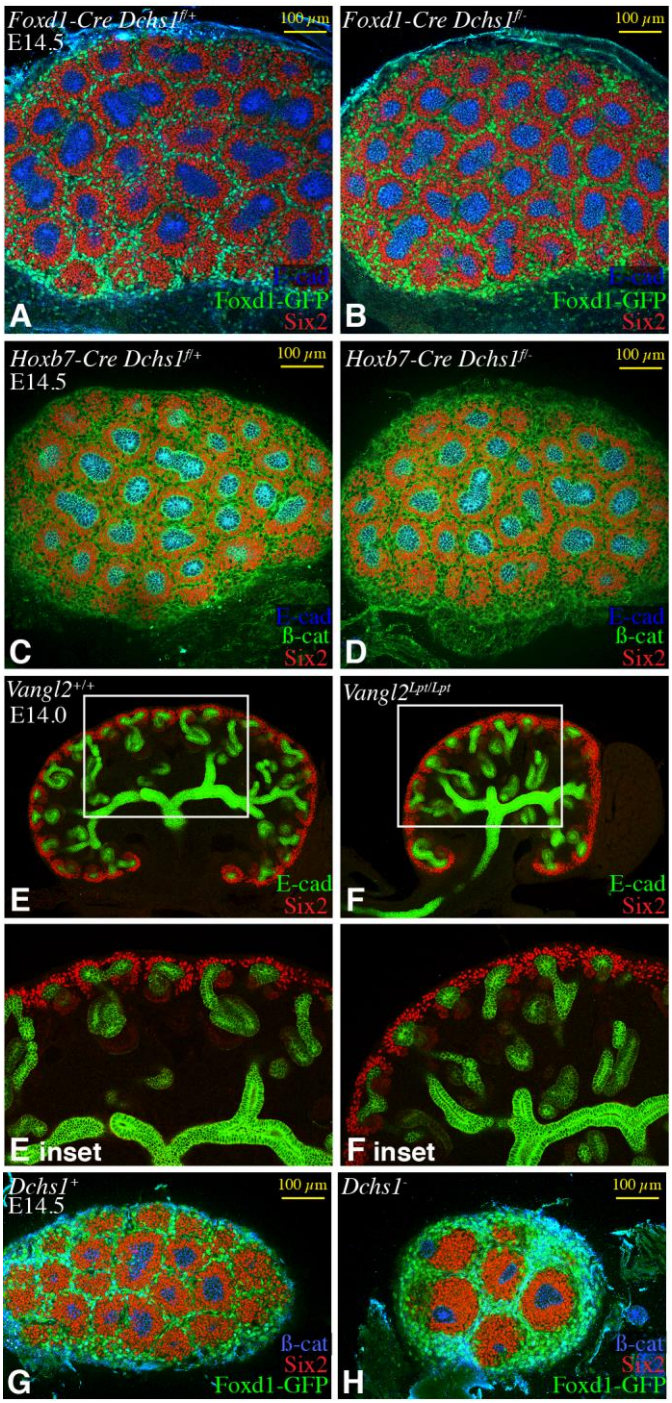

Figure S2. Lack of requirement for Dchs1 in stroma or UB

Embryonic kidneys stained for Six2 (red) to reveal CM, together with E-cad (blue, expressed in UB), and either ß-cat (green, expressed in all cells) or GFP (green). Scale bar (yellow) is 100 μm. A,B) Surface sections of E14.5 kidney from sibling control (A, Foxd1-Cre Dchs1$^{f/+}$), or mouse with conditional deletion of Dchs1 in stroma (B, Foxd1-

Cre Dchs1$^{f/-}$). C,D) Surface sections of E14.5 kidney from sibling control (C, Hoxb7-Cre Dchs1$^{f/+}$), or mouse with conditional deletion of Dchs1 in UB (D, Hoxb7-Cre Dchs1$^{f/-}$). E,F) E14.0 *Vangl2*^{Lpt} (F) and wild-type sibling (E), stained for E-cad (green) and Six2 (red). Lower panels (-inset) show higher magnifications of the boxed regions. (G,H) Surface section through sibling control (G) and *Dchs1*$^{-/-}$ (H) E14.5 kidneys imaged for ß-cat (blue), Six2 (red), and Foxd1-GFP (green).

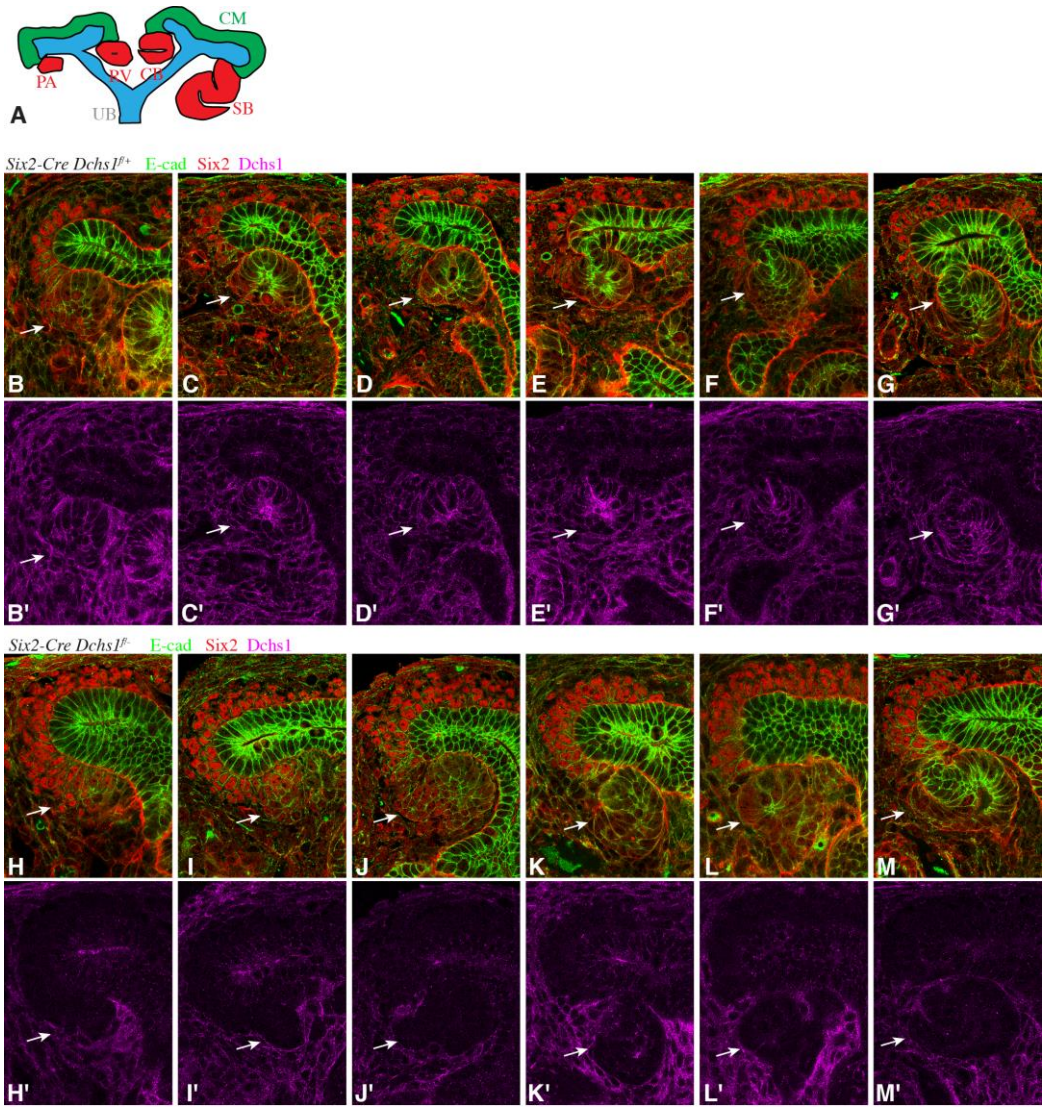

Figure S3. Abnormal initiation of nephrogenesis after conditional deletion of Dchs1 in CM

A) Schematic illustrating progressive stages of early nephrogenesis, from PA (pre-cellular aggregate) to RV (renal vesicle) to CB (comma shaped body) to SB (S shaped body). B-M) Examples from sibling controls (B-G, *Six2-Cre Dchs1$^{f/+}$*) or kidneys with conditional deletion of Dchs1 in CM (H-M, *Six2-Cre Dchs1$^{f/-}$*), stained for E-cad (green), Six2 (red), and Dchs1 (magenta, in panels marked by prime symbols). Several examples

are shown because the defects are heterogeneous. White arrows indicate the forming PA/RV/CB. Defects visible here include persistence of strong nuclear Six2 expression on the proximal side of the UB (H,I), irregular size and shape of the RV/CB (J-M, cf C-G), and irregular location and orientation of connecting tubules (L,M, cf E-G), see also Fig. 4. Dchs1 staining in A-G reveals distinct apical accumulation of Dchs1 in RV. Lack of Dchs1 staining in H-M identifies CM derivatives even after Six2 expression declines.

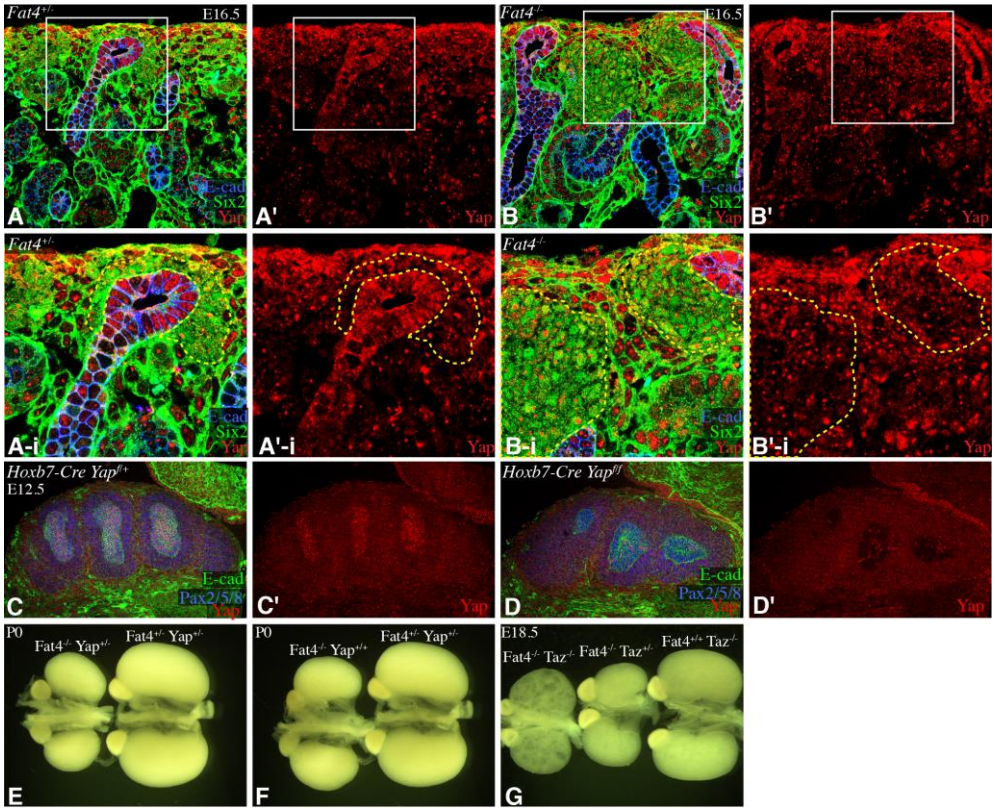

Figure S4. Lack of interaction of *Fat4* mutation with Yap or Taz

A,B) Confocal images of E16.5 kidneys stained for Yap using tyrimide signal amplification (red), Six2 (green), E-cad (blue). The Six2 antisera used here has high non-specific background, but Six2-specific staining is nuclear. The boxed regions are shown at high magnification below (panels labeled by "i"). Prime symbols identify panels with only a subset of stains shown. Dashed yellow line outlines CM, which shows similar levels of heterogeneous Yap nuclear stain in wild-type and mutants. C,D) Whole E12.5 kidneys stained for Yap (red) Pax2/5/8 (blue) and E-cad (green) for confirmation of Yap antisera specificity, from sibling control (C, Hoxb7-Cre $Yap^{f/+}$), or mouse with conditional deletion of Yap in UB (D, Hoxb7-Cre $Yap^{f/f}$). E-G) Whole kidneys from mice with combinations of *Fat4*, *Yap*, and *Taz* alleles. E) Comparison of P0 kidneys from $Fat4^{-/-}$ $Yap^{+/-}$ and $Fat4^{+/-}$ $Yap^{+/-}$ siblings. F) Comparison of P0 kidneys from $Fat4^{-/-}$ $Yap^{+/+}$ and $Fat4^{+/-}$ $Yap^{+/-}$ siblings. G) Comparison of E18.5 kidneys from $Fat4^{-/-}$ $Taz^{-/-}$, $Fat4^{-/-}$ $Taz^{+/-}$, $Fat4^{+/+}$ $Taz^{-/-}$ siblings.